1
Old and New Things in Thermoelectricity

Rudolf P. Huebener

The three thermoelectric phenomena, which are associated with the names Seebeck, Peltier, and Thomson and are due to the simultaneous presence of an electric field and a temperature gradient in a material, have been studied for almost 200 years. In 1821, Thomas Johann Seebeck discovered the effect named after him. This effect appears if two different electric conductors A and B are connected as shown in Figure 1.1a and if the two junctions are kept at different temperatures T_1 and T_2. In this case, a thermoelectric voltage develops in the circuit, which can be measured between the two ends of the conductor A. The Peltier effect shows up if two conductors A and B are connected in series and are kept at uniform temperature (Figure 1.1b). If an electric current of density J passes through the two conductors, heat will be generated or absorbed at the junction depending on the current direction and the junction area will be heated or cooled. The Peltier effect was discovered in 1834 by Jean Charles Athanase Peltier. The third thermoelectric effect occurs if an electric current of density J flows in an electric conductor in which a temperature gradient exists along the current direction (Figure 1.1c). This effect was predicted theoretically in 1854 and observed experimentally in 1856 by William Thomson, also known as Lord Kelvin. In the following, we look a bit closer at these thermoelectric phenomena. A more detailed treatment of these subjects has been given earlier by the author [1].

Thermoelectric Bi_2Te_3 Nanomaterials, First Edition.
Edited by Oliver Eibl, Kornelius Nielsch, Nicola Peranio, and Friedemann Völklein.

1.1
Three Thermoelectric Effects

1.1.1
Seebeck Effect

The thermoelectric voltage ΔV developed between the two ends of conductor A, shown in Figure 1.1a, increases proportionally to the temperature difference ΔT between the two junctions. The derivative

$$\frac{dV}{dT} = S_{\mathrm{AB}} \equiv S_{\mathrm{A}} - S_{\mathrm{B}} \tag{1.1}$$

is defined as the thermoelectric power S_{AB} of conductor A relative to that of conductor B. S_{A} and S_{B} are the absolute thermoelectric power of the two conductors, respectively. From Figure 1.1a and Equation 1.1, we see that the Seebeck effect vanishes because of symmetry reasons if conductors A and B are identical.

The Seebeck effect results from the general mechanism of thermal diffusion of particles in a temperature gradient. In the presence of the temperature gradient dT/dx the thermal force $-S_{\mathrm{tr}} dT/dx$ acts on the particles. The quantity S_{tr} is the transport entropy of the particles. In an electric conductor, this leads to the accumulation of opposite electric charges at the two ends of the conductor, which in turn causes an electric field E_x. At equilibrium, the thermal force is compensated by the electrostatic force q E_x, where q is the (positive or negative) electric charge. The forces satisfy the equation

$$-S_{\mathrm{tr}} \frac{dT}{dx} = qE_x = -q\frac{dV}{dx} \tag{1.2}$$

From Equation 1.2, we find the thermoelectric power S (also referred to as the Seebeck coefficient):

$$S \equiv \frac{dV}{dT} = \frac{S_{\mathrm{tr}}}{q} \tag{1.3}$$

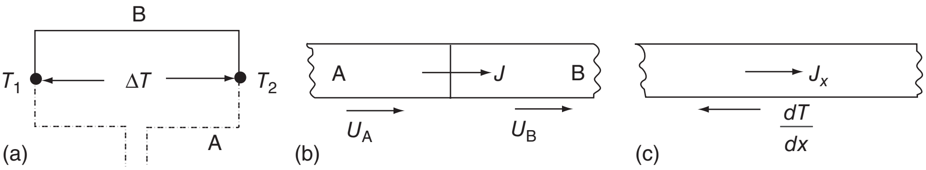

Figure 1.1 The thermoelectric effects: (a) Seebeck effect, (b) Peltier effect, and (c) Thomson effect.

1.1.2
Peltier Effect

The Peltier effect (Figure 1.1b) simply results from the fact that an electric current always transports thermal energy also. Denoting the heat current density as U_x, which is carried by the electric current density J_x, the ratio of the two is defined as the absolute Peltier coefficient π of the material:

$$\pi = \frac{U_x}{J_x} \tag{1.4}$$

The net Peltier heat appearing at the junction between two conductors A and B is given by $\pi_{\mathrm{AB}} \equiv \pi_{\mathrm{A}} - \pi_{\mathrm{B}}$. π_{AB} is positive if heat is generated at the junction when the current flows from A to B.

1.1.3
Thomson Effect

This effect occurs if a current flows in an electric conductor in which a temperature gradient is maintained along the current direction (Figure 1.1c). The rate of heat generation per volume in the conductor is

$$\frac{dQ}{dt} = \frac{J_x^2}{\sigma} + \frac{d}{dx}\left(\kappa\,\frac{dT}{dx}\right) - \mu J_x \frac{dT}{dx} \tag{1.5}$$

Here, σ and κ are the electric conductivity and the heat conductivity, respectively. μ is the Thomson coefficient. On the rhs, the first term represents the irreversible Joule heat, whereas the second term contains the divergence of the heat current density. The third term, which is linear in J_x and dT/dx, describes the Thomson effect and represents reversible generation or absorption of heat. While the Seebeck and Peltier effect can only be observed between two different materials, the Thomson effect can be measured directly for one homogeneous material.

Thomson already recognized that the absolute thermoelectric power S, the Peltier coefficient π, and the Thomson coefficient μ are related to each other, and from thermodynamic arguments he derived the following equations:

$$\mu = T\frac{dS}{dT} \tag{1.6}$$

and

$$\pi = TS \tag{1.7}$$

Subsequently, Lars Onsager has shown that Equations 1.6 and 1.7 follow directly from the theory of irreversible thermodynamics and his famous reciprocity relations.

From Equation 1.6 we find

$$S(T) - S(0) = \int_0^T \frac{\mu}{T}\, dT \tag{1.8}$$

Because of the third law of thermodynamics, we have $S(0) = 0$ and therefore

$$S(T) = \int_0^T \frac{\mu}{T}\, dT \tag{1.9}$$

Relation (1.9) allows in principle to find the absolute value of the Seebeck coefficient $S(T)$ if the Thomson coefficient $\mu(T)$ has been measured.

1.2
Semiconductors

Because of the large concentration of electric charge carriers in metals and alloys, their Fermi energy ε_F is relatively high, and near room temperature and below the charge carriers represent a degenerate Fermi gas. As a result, only a small fraction of the charge carriers with energies near ε_F can participate in the electric transport phenomena. This fraction is given by the reduction factor $k_\mathrm{B}T/\varepsilon_\mathrm{F}$, where k_B is the Boltzmann's constant. In the case of the monovalent metals, near room temperature we have approximately $k_\mathrm{B}T/\varepsilon_\mathrm{F} \approx 0.01$. Therefore, for thermoelectric cooling in particular, metals are generally not attractive. In the case of semiconductors this is quite different.

The small concentration of charge carriers in a semiconductor results in a small value of the Fermi energy ε_F, and at not too low temperatures we have $\mathrm{k_B}\ T \gg \varepsilon_\mathrm{F}$. Therefore, the Fermi distribution is replaced by the classical Boltzmann distribution

$$f = e^{-(\varepsilon - \varepsilon_F)/k_B T} \tag{1.10}$$

and the reduction factor $k_\mathrm{B}T/\varepsilon_\mathrm{F}$ does not show up in the transport phenomena. In the case of doped semiconductors the Seebeck coefficient S_n (S_p) for n-doping (p-doping) is

$$S_n = -\frac{k_\mathrm{B}}{|e|}\left[\left(\frac{5}{2} + r\right) + \frac{\varepsilon_\mathrm{C} - \varepsilon_\mathrm{F}}{k_\mathrm{B}T}\right] \tag{1.11}$$

and

$$S_p = \frac{k_B}{|e|}\left[\left(\frac{5}{2} + r\right) + \frac{\varepsilon_F - \varepsilon_V}{k_B T}\right] \tag{1.12}$$

Here, ε_C is the energy of the lower edge of the conduction band and ε_V the energy of the upper edge of the valence band. |e| denotes the absolute value of the elementary charge. The quantity r is the exponent of the energy-dependent scattering time τ from the relation $\tau \sim \varepsilon^r$.

Since about half a century, semiconductors based on the Bi_2Te_3 system have been applied in particular for Peltier cooling. Doping with Se yields $Bi_2Te_{3-x}Se_x$ as the n-material and with Sb yields $Bi_{2-x}Sb_xTe_3$ as the p-material. In the 1950s, it was Abram Fedorovich Joffe who pointed out the great potential of semiconductors for thermoelectric cooling [2]. At that time, his optimistic view caused strong research activities in the field of semiconductors in many laboratories of the electronics industry.

Peltier cooling at the junction between an n-doped and a p-doped semiconductor is highly effective, since the heat energy according to $\pi_{AB} \equiv \pi_A - \pi_B$ extracted from the junction amounts to the *sum* of π_A and π_B due to the opposite sign of the two Peltier coefficients. Because of the Joule heating in the n- and p-doped semiconducting sections of the Peltier cooling system, at the cold end the temperature passes through a minimum as a function of the current (with the temperature on the warm end being fixed). Denoting the temperature on the warm and the cold ends by T_o and T_1, respectively, the maximum temperature drop $(T_o - T_1)_{max}$ is [2]

$$(T_o - T_1)_{max} = \frac{1}{2} z\, T_1{}^2 \tag{1.13}$$

Here,

$$z = \frac{S^2}{\kappa\, \rho} \tag{1.14}$$

is referred to as the *figure of merit*, where S, κ, and ρ are the Seebeck coefficient, the heat conductivity, and the electric resistivity, respectively. In Equation 1.13 the figure of merit z is assumed to be constant in the temperature range between T_0 and T_1. From Equation 1.13 one finds

$$(T_0 - T_1)_{max} = \frac{1}{2z}\left[(2zT_0 + 1)^{1/2} - 1\right]^2 \tag{1.15}$$

Using the typical values near room temperature $S_n = -200\,\mu V/K$, $S_p = 200\,\mu V/K$, $\rho = 1\,m\Omega\,cm$, and $\kappa = 15 \cdot 10^{-3}\,W/cm\,K$, one obtains $z = 2.7 \cdot 10^{-3}\,K^{-1}$. This value of z together with Equation 1.15 and $T_0 = 283\,K$ yields $(T_0 - T_1)_{max} = 64\,K$.

1.3
My Entry into Thermoelectricity

In the early 1960s, there was a strong interest in the research on lattice defects in metals and alloys. This resulted in part from the upcoming field of nuclear engineering and the lack of knowledge about radiation damage. (e.g., regarding the use of graphite as moderator for the neutrons in a nuclear reactor, Eugene Wigner worried that possibly the carbon atoms would be removed from their regular sites in the graphite lattice by collisions with the energetic neutrons. In this way, a highly excited material similar to dynamite may be generated, releasing its stored energy perhaps abruptly by an explosion.) In addition, the goal of an improved understanding of the mechanisms leading to metal fatigue also played a role. In this context, lattice vacancies in crystals became an important subject for experimental and theoretical studies.

Lattice vacancies can be generated in a thin metallic wire by Joule heating the wire to temperatures near the melting point by passing an electric current through it and then cooling the wire rapidly by dropping it into ice water. By such quenching experiments, lattice vacancies (generated under thermodynamic equilibrium at the high temperatures) are frozen into the wire. Cooling rates of about $2 \cdot 10^4$ K/s can be achieved [3]. Subsequently, the changes in the sample properties can be investigated.

I fabricated a thermocouple of two gold wires of 0.254 mm diameter, of which one wire contained lattice vacancies due to quenching from a high temperature, whereas the other wire was well annealed [3]. From the voltage output of this thermocouple the change ΔS of the Seebeck coefficient due to the vacancies could be determined. It is shown in Figure 1.2 as a function of temperature. The change ΔS is given by the sum of the change ΔS_e of the electronic component, S_e, and the change ΔS_g of the phonon-drag component, S_g, [3]

$$\Delta S = \Delta S_\mathrm{e} + \Delta S_\mathrm{g} \tag{1.16}$$

(The phonon-drag component S_g of the thermo-power is caused by the interaction of the phonon current in a temperature gradient with the electrons. It is an effect of first order, and it can dominate in some temperature ranges). As explained in Ref. [3], in the case of gold the two components $\Delta S_\mathrm{e}(T)$ and $\Delta S_\mathrm{g}(T)$ can be obtained separately, if $\Delta S(T)$ is measured between 4.2 K and room temperature. One interesting result was that the change $\Delta S_\mathrm{g}(T)$ indicated that the vacancies caused strong phonon scattering, associated mainly with their strain field.

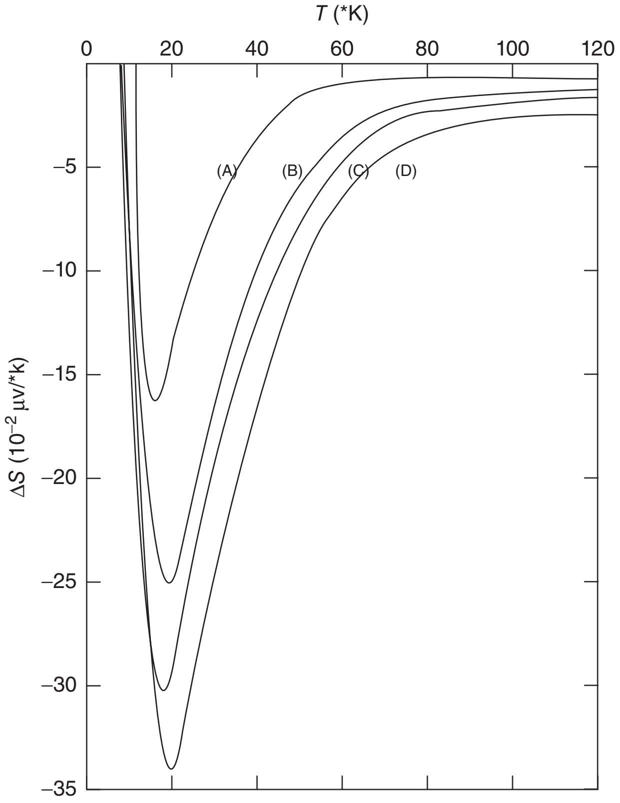

Figure 1.2 Change of the absolute thermoelectric power of gold caused by quenched-in vacancies as a function of temperature for different vacancy concentrations c [3]. (a) $c = 0.403 \cdot 10^{-2}$ at%; (b) $c = 0.825 \cdot 10^{-2}$ at%; (c) $c = 0.865 \cdot 10^{-2}$ at%; and (d) $c = 1.42 \cdot 10^{-2}$ at%.

The influence of the specimen size and of surface scattering represents another interesting subject. By fabricating a thermocouple simply from a wire and a very thin foil strip of exactly the same material, this size effect can be measured directly. I have performed such experiments by fabricating a thermocouple from gold wire of 0.254 mm diameter and strips of various gold foils with thickness ranging from $1.5 \cdot 10^{-3}$ to $2.5 \cdot 10^{-2}$ mm [4]. Since the output of these thermocouples was expected to be very small, the thermoelectric voltage was measured just by keeping the hot junction at room temperature and by placing the cold junction in liquid nitrogen (77 K). The result is shown in Figure 1.3. These data were obtained by dividing the thermoelectric voltage by the temperature difference between the

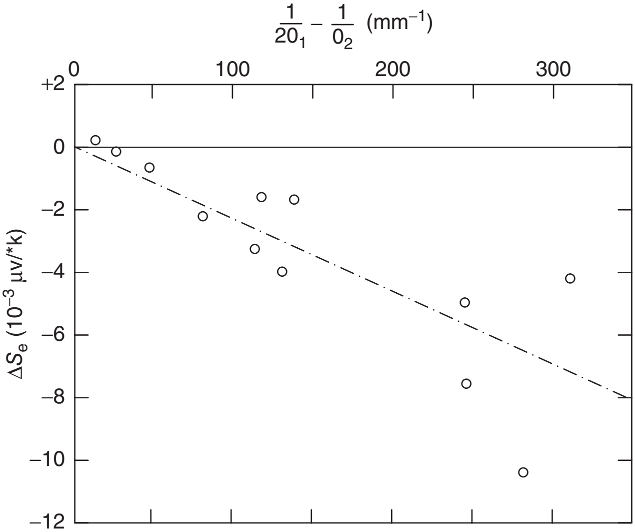

Figure 1.3 Difference between the thermoelectric power of a gold foil of thickness a_1 and a gold wire of diameter $a_2 = 0.254$ mm in the temperature range between 77 and 296 K [4].

hot and the cold junction, hence representing average values in this temperature regime. Since in gold phonon-drag effects vanish above about 100 K [3], the phonon-drag contribution ΔS_g is negligible.

The difference between the electronic component of the thermo-power of a foil of thickness a_1 and a wire of diameter a_2 is [4]

$$\Delta S_e \equiv S_e^{\text{foil}} - S_e^{\text{wire}} = \left(\frac{1}{2a_1} - \frac{1}{a_2}\right) \frac{\pi^2 k_B^2}{4|e|} \frac{T\,\ell}{\varepsilon_F} \left\{\frac{\partial \ln \ell(\varepsilon)}{\partial \ln \varepsilon}\right\}_{\varepsilon_F} \tag{1.17}$$

Here ℓ denotes the electron mean free path. Using Equation 1.17, the value

$$\left\{\frac{\partial \ln \ell(\varepsilon)}{\partial \ln \varepsilon}\right\}_{\varepsilon_F} = -0.53 \pm 0.19 \tag{1.18}$$

was calculated from the data of Figure 1.3 [4]. Such a decrease in the electron mean free path with increasing energy is expected from theory.

The route from the thermal diffusion of charge carriers in electric conductors to the thermal diffusion of magnetic flux quanta in superconductors is not far. In the 1960s, the phenomenon of the motion of magnetic flux quanta in the mixed and the intermediate state of superconductors quickly developed into an important subject. Owing to the thermal force effected by a temperature gradient, magnetic flux quanta move from the hot to the cold side of the specimen. As a consequence, an electric field oriented perpendicular to the directions of the temperature gradient and of the magnetic field is generated [5]. This is exactly the Nernst effect. By slightly modifying our experimental configuration and surrounding the cryostat by a small superconducting magnet, in the late 1960s we were able to perform some of the first experiments dealing with the Nernst effect in thin-film superconductors [6, 7]. (Flux motion due to the Lorentz force of an applied electric current is directed perpendicular to the current and results in a (longitudinal) electric field parallel to the current and in the phenomenon of flux-flow resistance [5].)

1.4
Peltier Cascades

Starting near room temperature, cooling to temperatures much lower than the value indicated from Equation 1.15 is possible by means of cascades of Peltier elements. We note that the maximum temperature drop of a single stage given by Equations 1.13 and 1.15 can only be reached if the heat load imposed on the cold side is zero. With increasing heat load the temperature drop $(T_0 - T_1)$ decreases linearly, reaching zero when the heat load is equal to half the electric power dissipated in the Peltier stage [2, 8]. Therefore, the higher stages in a Peltier cascade should become successively smaller. As an example, we give the following temperature values at the cold side of the different stages of a four-stage Peltier cascade with $T_0 = 283\,\mathrm{K}$ on the warm side of the first stage and for $z = 3 \cdot 10^{-3}\,\mathrm{K}^{-1}$ [8]: stage 1 – 228, K; Stage 2 – 189 K; Stage 3 – 161 K; Stage 4 – 134 K. Here, from one stage to the next a reduction in size by a factor of 10 is assumed. Further, the figure of merit z was taken as a constant over the whole temperature range of the cascade.

Experiments performed with a five-stage arrangement of commercially available Peltier modules reached 149 K on the cold end, with the temperature at the warm end being fixed at 282 K [8]. In order to reach lower temperatures by means of Peltier cascades, better thermoelectric materials must be developed.

1.5
Challenge of Materials Science

Since about 60 years, the Bi_2Te_3 system with the n- and p-doped compounds indicated above has been the dominating material for applications in the Peltier cooling technology. During this time the quantity zT at room temperature could be increased only from about 0.6 to 1.0. For some time there have been strong research efforts to increase zT appreciably above this value of 1.0. Presently, this goal represents an important challenge for materials science. In 1993, Hicks and Dresselhaus proposed that quantum-well structures would be promising for appreciably increasing the figure of merit [9]. Their paper started a new and still ongoing round of research activities emphasizing in particular thin-film technology and advanced sintering techniques for materials preparation.

References

1. Huebener, R.P. (1972) in *Solid State Physics, Advances in Research and Applications*, vol. 27 (eds H. Ehrenreich, F. Seitz, and D. Turnbull), Academic Press, p. 63.
2. Joffe, A.F. (1957) *Semiconductor Thermoelements and Thermoelectric Cooling*, Infosearch, London.
3. Huebener, R.P. (1964) *Phys. Rev.*, **135**, A1281.
4. Huebener, R.P. (1964) *Phys. Rev.*, **136**, A1740.
5. Huebener, R.P. (2001) *Magnetic Flux Structures in Superconductors*, 2nd edn, Springer, Berlin.
6. Huebener, R.P. (1967) *Phys. Lett.*, **24A**, 651; **25A**, 588.
7. Huebener, R.P. (1968) *Phys. Lett.*, **28A**, 383.
8. Huebener, R.P. and Tsuei, C.C. (1998) *Cryogenics*, **38**, 325.
9. Hicks, L.D. and Dresselhaus, M.S. (1993) *Phys. Rev. B*, **47**, 12727.